

Nonlinear Analysis of Human Atrial Flutter and Fibrillation Using Surface Electrocardiogram

T Kao¹, YY Su¹, HW Tso¹, YC Lin¹,
SA Chen², CT Tai²

¹Institute of Biomedical Engineering, National Yang-Ming University, Taipei, Taiwan, ROC

²Taipei Department of Cardiology, Veterans General Hospital, Taipei, Taiwan, ROC

Abstract

Atrial flutter and atrial fibrillation have different generating mechanisms in atrium. They are often cross-classified from the surface ECG. Nonlinear analysis has recently been applied to electrograms, and atrial arrhythmia is shown evidence that indicates the possibility of deterministic chaos. In this study, we applied methods from the theory of nonlinear dynamics to characterize electrograms of atrial flutter and fibrillation in humans. For typical flutter, nonlinear parameters were relatively smaller, and they presented higher values when in Af. In atypical flutter, the magnitude of these nonlinear parameters was between those of typical flutter and Af. Statistical analysis showed evidence that they exhibited a significant differentiation allowing the classification of these arrhythmias. By using the neural network classification, a desirable result was also obtained. Therefore, nonlinear analysis provided us an advantageous technique to discriminate among typical flutter, atypical flutter and Af electrograms from surface ECG.

1. Introduction

Atrial flutter (AFL, including typical and atypical) and atrial fibrillation (Af) are two of the most common cardiac arrhythmias. During AFL and Af, atrial activity appears disordered and loses its regular rhythm. Typical flutter, atypical flutter and Af have different generating mechanisms in the atrium. On ECG, typical flutter has apparent saw-toothed P waves and regular cycle length. Atypical flutter, which is unstable and often degenerates into Af, has more variable ECG pattern than typical flutter. Af shows chaotic f waves. Due to there being no strict definitions of atrial rate and atrial morphology in ECG, they are often cross-classified from the surface ECG. Nonlinear analysis has recently been applied to cardiac signals, and atrial arrhythmia has shown evidence that indicates the possibility of deterministic chaos. In nonlinear dynamical systems, several characteristics can be used to describe the system, including correlation

dimension, largest Lyapunov exponents, Kolmogorov entropy, complexity, etc. and they have been used to explain ECG signal behavior in many studies. Therefore, we attempted to apply such technique to discriminate among typical flutter, atypical flutter and Af.

2. Methods

Twelve-lead ECG from twenty atrial flutter patients (ten typical flutters and ten atypical flutters) and seven Af patients at the Taipei Veterans General Hospital, Taipei, Taiwan were analyzed. ECG signals were acquired by Prucka program (Cardiolab system, Prucka GE, Marquette US) with a sampling rate of about 1000 Hz. MATLAB and TISEAN toolbox [1] were used to analyze the recorded ECG signals.

Independent component analysis (ICA) is a technique which can be used to extract the atrial activity from ECG [2]. The ICA model is

$$X = AS$$

where S is the source vector, X is the observations and A is an unknown mixing matrix. 12-lead ECG could be identified with X and complied with ICA model, where vector S comprised the independent sources of atrial and ventricular activity and other nuisance signals. First, signals were de-noised. Then, 12-lead ECG was separated into 9 to 12 sources by FastICA. Among these source components, we found several possible atrial sources according to their frequency spectra and kurtosis. By using inverse ICA, 12-lead atrial activity was reconstructed. ICA-estimated atrial activity had to be approximated to the real atrial signals. If ICA-estimated atrial activity was not approximated to the real atrial signals, we had to re-choose the atrial sources and reconstruct atrial activity again until the atrial activity was similar to the real atrial signals.

According to Taken's time-delay theorem, atrial signal $\{x(i)\}_{i=1}^L$ was used to reconstruct the dynamics, the so called phase space [3]. Delay vector $\vec{x}(i)$ was reconstructed in the phase space as

$$\vec{x}(i) = (x(i), x(i + \tau), x(i + 2\tau), \dots, x(i + (m-1)\tau))$$

where τ was the embedding delay and m was the embedding dimension of the reconstructed phase space. The embedding delay was chosen based on first minimum mutual information [4] and the embedding dimension was chosen according to false-nearest neighbor algorithm [5].

Grassberger-Procaccia (GP) algorithm [6] is the method used to measure the geometrical complexity of trajectory in the phase space. First, the correlation integral, which counts the number of neighbor points in phase space around the chosen reference point, is evaluated.

$$C_m(r, N, w) = \frac{2}{N(N-1)} \sum_{j=i}^N \sum_{i=j+w}^N \theta(r - |\vec{x}_i - \vec{x}_j|)$$

where $\theta(x) = 1$ when $x > 0$, $\theta(x) = 0$ when $x \leq 0$ and w (Theiler window) is set equal to twice the time delay. The correlation dimension is associated with the organization of points in phase space and is a measure of the geometrical complexity of the trajectory. The correlation dimension (D_m) at embedding dimension m is estimated from the slope in the scaling region by linear regression through points $(\log(r), \log C_m(r))$.

$$D_m(r) = \frac{d \log C_m(r)}{d \log(r)}$$

In case $D_m(r)$ saturates as a function of m , this value is taken as the correlation dimension D_2 .

Lyapunov exponents (λ), which are used to quantify the sensitivity of the system to initial conditions, are defined as the long-time average exponential rates of divergence of nearby states. Lyapunov spectrum can be estimated by Sano and Sawda [7]. Consider a small ball of radius ε , where $\varepsilon = 0.2 \times STD(x_i) \times \sqrt{m}$, centered at the orbital point $\vec{x}(k)$ in the phase space and find any set of points $\{\vec{x}(k_i)\}$ ($i = 1, 2, \dots, N_{neigh}$) included in this ball. All the displacement vectors $\Delta \vec{x}_k$ and $\Delta \vec{x}_{k+1}$ are computed, and the flow operator A_ε^k is obtained to minimize the square error from:

$$\Delta \vec{x}_{k+1} = A_\varepsilon^k \Delta \vec{x}_k$$

The computation involves a number of steps until convergence. After s steps, the Lyapunov spectrum estimate is given by

$$\lambda_i = \frac{1}{s \Delta t} \sum_{k=0}^{s-1} \ln \|A_\varepsilon^k \cdot e_i^k\|, \quad i = 1, 2, \dots, m$$

where e_i^k is a set of basis vectors of the tangent space at \vec{x}_k , m is the embedding dimension, and Δt is the time interval. For an m -dimension phase space, there

would be m Lyapunov exponents. λ_1 , the largest Lyapunov exponent, is regarded as an estimator of the dominant chaotic behavior of a system.

Lyapunov exponents quantify the expansion and contraction of the trajectories in phase space. Kolmogorov entropy (KE) is defined as the sum of all positive Lyapunov exponents in dynamics as follows:

$$KE = \sum_i \lambda_i, \text{ where } \lambda_i > 0$$

It quantifies the expansion of phase space volume, also the rate of the dynamical system losing its phase-space information and the dissipation of the dynamical system.

Complexity measure (C) is related to the number of steps in a self-delimiting production process of a sequence [8]. First, for every data point $\{x(i)\}_{i=1}^L$, the mean value was subtracted. Data were compared with a threshold $T_d = 0.2 \times STD(x_i)$. If $-T_d < x_i < T_d$, then $s_i = 0$, otherwise $s_i = 1$. Thus, ECG signals were transformed into a binary sequence which only consisted of the characters 0 or 1. Secondly, the Lempel-Ziv complexity algorithm, which uses two simple operations, comparison and accumulation, was evaluated to obtain the complexity of the signals.

The back-propagation network was used to classify in our study. The goal of the network was to correctly classify these three arrhythmias by the four nonlinear parameters. We used the results of eighteen patients as the training set data to construct the network and nine patients, which including 3 typical flutter, 3 atypical flutter and 3 Afs, as the test set data.

3. Results

3.1. Atrial activity extraction by ICA

Twelve-lead atrial activity was obtained from ICA algorithm. To verify the signals that we obtained exactly came from the atrium, the ICA-estimated atrial activities from leads II, aVF and V1 were compared with their original leads, respectively. In Figure 1, the ICA-estimated atrial activity is illustrated in red and the original surface ECG is in blue. It is observed that the ICA-estimated atrial activity corresponds to its projection onto the original ECG lead.

The signals of lead V1 that we analyzed are shown in Figure 2. From the atrial activity morphology and their dominant frequencies, it was still difficult to discriminate among these three types of arrhythmias.

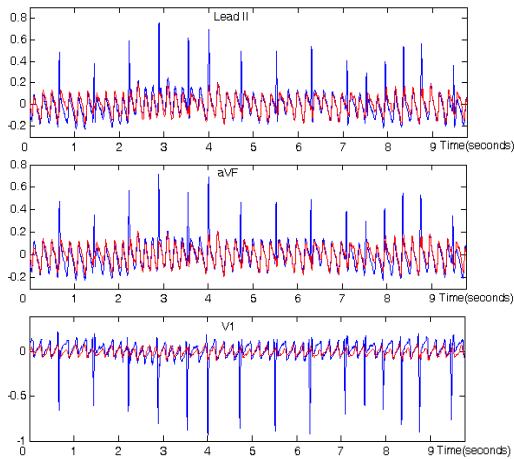


Figure 1. The ICA-estimated atrial activities from leads II, aVF and V1 were compared with their original leads, respectively. Upper: Lead II; Middle: Lead aVF; Lower: Lead V1.

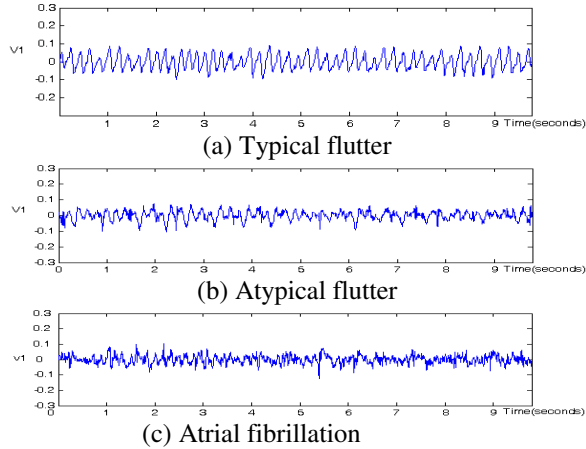


Figure 2. The ICA-estimated atrial activity of lead V1.

3.2. Nonlinear parameters

In these three types of arrhythmias, for typical flutter, nonlinear parameters were relatively smaller. D_2 , λ_1 , KE, and C ranged from 1.76 to 4.36, 0.06 to 6.92, 0.06 to 9.74, and 84 to 115, respectively. For Af, ECG patterns became chaotic and these parameters presented higher values. D_2 , λ_1 , KE, and C ranged from 4.56 to 6.34, 11.06 to 20.58, 15.63 to 33.05, and 124 to 158, respectively. During atypical flutter, ECG showed more complex than typical flutter but more regularity than Af and thus the magnitude of these nonlinear parameters presented between typical flutter and Af. The difference between typical flutter and Af was distinct and could be distinguished clearly. Next, statistics of nonlinear parameters in these three types of arrhythmias were evaluated as below to prove the differentiation among

them.

3.3. Statistical analysis

First, Kruskal-Wallis test was used. P-values of nonlinear parameters among these three types of arrhythmias were all smaller than 0.05. This confirmed that three different arrhythmias were statistically differentiated by using these four nonlinear features. Also, Mann-Whitney test showed that among these three types of arrhythmias there was statistical differentiation between any two of them ($P < 0.017$).

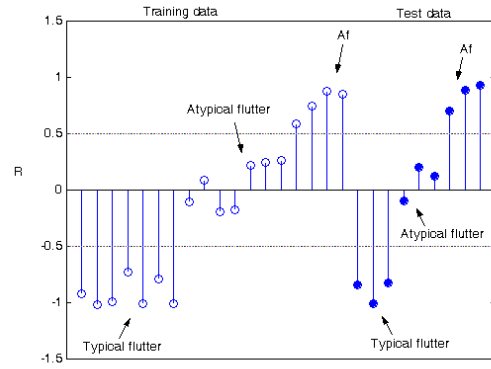


Figure 3. A neural network classification for training set data and test set data.

3.4. Neural network classification

After the network was generated from training data set, training and test set data were used to test the classification. The results of thirty classifications by neural network showed that most patients have a classification that matched the diagnosis. Figure 3 shows one of the results in neural network classification. In Figure 3, empty circles represent the results of training set data and full circles are the test set data. The training target of typical flutter was set as -1, atypical flutter as 0 and Af as 1. After testing, the results (R) of training set data showed that R of typical flutters were near -1, atypical flutter near 0 and Af near 1. The criteria of classification was set as follows: cases were classified as typical flutter when R was smaller than -0.5, as atypical flutter when R was between -0.5 and 0.5, and as Af when R was larger than 0.5.

The error of classification was about 1.48%. Therefore, according to the distribution of nonlinear characteristics, statistical test and neural network classification, it was confirmed that nonlinear characteristics provided us a good technique to discriminate these three types of arrhythmias.

4. Discussions

Adaptive noise canceller (ANC) is a technique to cancel ventricular activity in ECG. ANC was also used in our study. From the results, we found that after QRS-T complex subtraction in Af, atrial activity was approximate to lead V1. However, during typical and atypical flutter, it was difficult to choose a proper QRS-T template and undesirable results were obtained. Due to this reason, ICA technique was used to extract the atrial activity, and we found it had better performance.

Spectral analysis is a useful technique in discriminating the different atrial ECG signals. The results show that the dominant frequencies of typical flutter, atypical flutter and Af were 3.25 to 5, 4 to 7, and 5.38 to 7.63, respectively. It showed the tendency that Af had the highest frequency and typical flutters were the lowest. However, it was still difficult to distinguish these three types of arrhythmias from their dominant frequencies.

To estimate the correlation dimension, additional reconstruction parameters were chosen. In the curve of correlation dimension, it didn't appear plausible in each individual ECG. Therefore, a compromise was made between the choice of an embedding dimension and a suitable coarse-grained resolution. According to FNN and Taken's theorem, an 8-dimension was sufficient when in arrhythmia. Also, we chose a coarse-grained resolution equal to the standard deviation of the ECG divided by its peak-to-peak value. We did not claim that the choice of parameters was optimal in any sense. However, the choices made led to a procedure to discriminate among ECGs of these different arrhythmias. How to choose the reconstruction parameters optimally for time series remains a question worth investigating.

When evaluating complexity measure, the threshold for translating ECG signal into 0-1 string was crucial to judge the differences among those signals. In our study, the common threshold was chosen as $T_d = 0.2 \times STD(x_i)$. It led to some immunity from low-level noise and allowed us to adapt every ECG if there were any changes in the signal character. The selection of threshold was considered a property of data that we analyzed. The criteria of threshold could not promise useful in distinguishing other different signals.

5. Conclusions

Nonlinear analysis to discriminate different types of arrhythmias has been presented in this study. Four nonlinear parameters were evaluated to characterize and classify the surface ECG of typical flutter, atypical flutter and Af. The results showed that during Af, nonlinear parameters concentrated on higher values, were lower at typical flutter and between in atypical flutter. Statistical

analysis showed evidence that these parameters exhibited significant differentiation, allowing the classification of these arrhythmias. Neural network technique was then used to examine the accuracy of classification and we obtained a desirable result. In summary, nonlinear analysis provides us an advantageous technique to discriminate different types of ECG abnormality.

Acknowledgement

This study was supported by research grant (NSC92-2218-E-010-002) from the National Science Council, Taiwan, ROC.

References

- [1] Hegger R, Kantz H, Schreiber T. The TISEAN package, Time series methods: practical implementation of nonlinear. *Chaos*, 1999, 9:413-435.
- [2] Rieta JJ, Millet J, Zarzoso V, Castells F, Sanchez C, Garcia R, Morell S, Atrial fibrillation, atrial flutter and normal sinus rhythm discrimination by means of blind source separation and spectral parameters extraction. *IEEE Computers in Cardiology*, 2002, 25-28.
- [3] Hoekstra BPT, Diks CGH, Allesie MA, DeGoede J, Nonlinear analysis of epicardial atrial electrograms of electrically induced atrial fibrillation in man, *J. Cardiovasc. Electrophysiol.* 1995, 6:419-440.
- [4] Fraser AM, Swinney HL. Independent coordinates for strange attractors from mutual information. *Phys. Rev. A.*, 1985, 33: 1134-1140.
- [5] Kennel MB, Brown R, Abarbanel HI, Determining embedding dimension for phase-space reconstruction using a geometrical construction. *Phys. Rev. A.* 1992, 45: 3403-3411.
- [6] P. Grassberger, T. Schreiber, C. Schaffrath, "Nonlinear time sequence analysis," *Int. J. Bif. Chaos*, 1991, 1: 521-547.
- [7] Sano M, Sawada Y, Measurement of the Lyapunov spectrum from a chaotic time series," *Phys. Rev. Lett.*, 1985, 55: 1082-1085.
- [8] Lempel A, Ziv J, On the complexity of finite sequence. *IEEE Trans. Inform. Theory*, 1976, IT22: 75-81.

Address for Correspondence.

Tsair Kao
Institute of Biomedical Engineering
National Yang-Ming University
Taipei, 112 Taiwan
E-mail: tskao@ym.edu.tw